ELSEVIER

Polymer 42 (2001) 2365–2372

polymer

www.elsevier.nl/locate/polymer

Catalytic radical polymerization of vinyl monomers by cobalt porphyrin complex and metamorphosis of block-into-block copolymer

A.K. Nanda*, K. Kishore

Department of Inorganic and Physical Chemistry, Indian Institute of Science, Bangalore 560012, India

Received 7 March 2000; received in revised form 30 June 2000; accepted 18 July 2000

Abstract

This is the first report on the catalytic room temperature free-radical polymerization of vinyl monomers, namely styrene (STY) and methyl methacrylate (MMA) using Co(II)TPP(Py) and aerial oxygen as a catalyst and a co-catalyst, respectively. The mechanism of polymerization has been investigated using ^{1}H NMR, differential scanning calorimeter (DSC), thermogravimetric (TGA) and gel permeation chromatography (GPC) analysis and a radical pathway for the polymer formation is proposed. The rate of polymerization for the synthesis of active polymers of STY is higher than that of MMA, which has also been supported by computational studies. The active polymer, polystyrene (PS)–poly(styrene peroxide) (PSP) was also used for the synthesis of another block copolymer, PS-*b*-PMMA, by reacting PS–PSP with MMA. The mechanism of block copolymerization is discussed.

Keywords: Catalytic; Active polymers; Block copolymer

1. Introduction

Free-radical polymerization is one of the most important commercial processes leading to high molecular weight polymers, since a wide variety of monomers can be polymerized and copolymerized under relatively simple experimental conditions [1]. In this method, oxygen is always known to play the role as an inhibitor [2–4], until Tatsukami et al. [5] discovered that it is also an initiator for the polymerization of ethylene. Despite air being a major resource of oxygen, it has not been exploited for its initiating characteristics.

This is the first report on the room temperature free-radical polymerization of vinyl monomers, namely styrene (STY) and methyl methacrylate (MMA), achieved using the abundantly available oxygen as a co-catalyst and 5,10,15,20-tetraphenyl-21H,23H-porphyrine cobalt(II) pyridine {Co(II)TPP(Py)} complex as a catalyst. There are some reports in the literature on the low-temperature vinyl polymerization by redox initiation using Fe(II)/Co(II) salts but in a different context. For example, salts of Fe(II)/Co(II) have been used along with organic peroxides as redox initiators for polymerization. However, the metal salt gets consumed during the course of polymerization [6–9] unlike in the present method, where the Co(II)TPP(Py) catalyst is regenerated.

Interestingly, we have synthesized active polymers, namely polystyrene (PS)–poly(styrene peroxide) (PSP) and poly(methyl methacrylate) (PMMA)–poly(methyl methacrylate peroxide) (PMMAP) using Co(II)TPP(Py) in a single step, which is rather unusual in free-radical polymerization. Further, the transformation of a block copolymer macroinitiator like PS–PSP into another block copolymer namely PS-*b*-PMMA has been carried out, which seems rather novel. The molecular design of these active polymers and block copolymers has been one of the major topics of interest in polymer science during the last decade. Synthesis of block copolymers with structures such as AB or ABA type are important since many applications require a combination of the desired properties in one material [10–12]. In particular, diverse applications have been found for active polymers and block copolymers in the polymer industry. For example, block copolymers can be utilized either by themselves as high-performance polymers or can be added as surface modifier for polymeric materials or as compatibilizer for mechanical blends of two immiscible polymers [13,14].

---

* Corresponding author. Tel.: +91-80-3092382; fax: +91-80-3341683.
E-mail address: ajaya@ipc.iisc.ernet.in (A.K. Nanda).

0032-3861/01/$ - see front matter © 2000 Elsevier Science Ltd. All rights reserved.
PII: S0032-3861(00)00587-5

2. Experimental section

2.1. Materials

STY and MMA were freed from inhibitor and distilled under reduced pressure prior to use. 5,10,15,20-Tetraphenyl-21H,23H-porphyrin cobalt(II) {Co(II)TPP} (Aldrich) was used as received. Oxygen of high purity was used. Pyridine (Py), petroleum ether, methanol, chlorobenzene, ethyl acetate, chloroform, cyclohexane and acetonitrile were purified as reported previously [15].

2.2. Preparation of Co(II)TPP(Py) complex

Co(II)TPP(Py) complex was prepared by mixing solutions of equimolar concentrations (5.5×10^{-5} mol l^{-1}) of Co(II)TPP and Py in a vinyl monomer. The formation of Co(II)TPP(Py) is noted by the disappearance of peaks at 413 nm (soret peak) and 528 nm (Q peak) and the appearance of new peaks at 440 and 553 nm in the UV–visible (UV–VIS) spectra [16].

2.3. Preparation of PS–PSP and PMMA–PMMAP ‘active’ polymers

The polymerizations have been carried out in 10-ml flasks by taking a 5-ml solution of Co(II)TPP(Py) (5.5×10^{-5} mol l^{-1}) in a vinyl monomer (STY or MMA). The mouths of the flasks were tightly closed and kept in a vacuum desiccater in order to prevent exposure to air. However in the 10-ml flask, 5 ml of the solution was present and the remaining portion was air. All the polymerizations were carried out at room temperature. At different time intervals, the active polymers, polystyrene–poly(styrene peroxide) (PS–PSP) and poly(methyl methacrylate)–poly(methyl methacrylate peroxide) (PMMA–PMMAP) were precipitated using petroleum ether as a non-solvent, and further purified by repeated precipitation from chloroform and dried in vacuum at ambient temperature to a constant weight.

2.4. UV–visible studies

The UV–VIS spectra were recorded to study the nature of the cobalt catalyst before and after the polymerization. The UV–VIS spectra of Co(II)TPP(Py) adduct in the monomer remains unaffected with the same absorbance after the polymerization reaction. It indicates that Co(II)TPP(Py)$^{-}$OO$^{\cdot}$ adduct after an electrophilic addition reaction with the monomer regenerates back to Co(II)TPP(Py) and does not undergo irreversible oxidation under the present reaction condition.

2.5. Preparation of PS-b-PMMA block copolymer

The PS–PSP active polymer and MMA were taken in pyrex ampoules, which were previously sealed after repeated freeze–thaw-cycles in liquid nitrogen. One of the sealed ampoules was kept at room temperature for 5 days and others were kept at 80°C for 5 h. The polymers were precipitated using methanol as a non-solvent, and further purified by repeated precipitation from chloroform, and dried under vacuum at 50–70°C for 15 h.

2.6. Purification of PS-b-PMMA

Homopolymers of STY and MMA obtained as by-products in the synthesis of PS-*b*-PMMA were purified by solvent extraction. The polymer was extracted with cyclohexane for 80 h by Soxhlet extractor to extract PS using cylindrical filter paper. The dried residue was extracted with acetonitrile for 80 h to extract PMMA. The remaining polymer was extracted with benzene for 80 h to obtained PS-*b*-PMMA. The extracts were concentrated by evaporating the excess solvent using a rotary evaporator (Yamato Hi Tec, Model RE-51) and they were then added to 300 ml of methanol to precipitate each polymer.

2.7. Techniques

The ^{1}H NMR spectra in CDCl$_3$ were recorded on a Bruker ACF 200 MHz spectrometer using tetramethyl silane as an internal standard. The UV–VIS spectra were taken on a Hitachi instrument, Model U-3400. Differential scanning calorimeter (DSC) analyses were performed on a Perkin–Elmer DSC-7 at a heating rate of 10°C/min in a flowing nitrogen (30 cm^{3}/min) atmosphere. Thermogravimetric (TG) analysis was carried out on a Perkin–Elmer TGS-2 instrument under nitrogen atmosphere at a heating rate of 5°C/min. The number average molecular weights ($\bar{M}_{\mathrm{n}}$) and weight average molecular weights ($\bar{M}_{\mathrm{w}}$) and polydispersity index ($\bar{M}_{\mathrm{w}}/\bar{M}_{\mathrm{n}}$) were estimated using gel permeation chromatography (GPC). The GPC was performed on a modular system consisting of a Waters 590 HPLC pump, a Waters 717 autosampler (Waters Corporation, Milford, MA) and an ERMA ERC-7515A refractive index detector (ERMA CR Inc., Tokyo). The column used was a 60-cm PLGel mixed-B 10-micron column (Polymer Laboratories Ltd, Shropshire, UK). The mobile phase used was unstabilized THF (EM Science, Gibbstown, NJ) at a flow rate of 0.95 ml/min. The molecular weights were calculated using 13 narrow polystyrene standards from 6,300,000 to 580 (Pressure Chemical Co., Pittsburgh, PA). The software used for the calculations was PL CALIBER version 7.04 (Polymer Laboratories Ltd, UK).

3. Computational studies

The quantum mechanical semiempirical program packages MOPAC and VAMP version 6.0 were used for computations [17]. The geometry of the radicals was fully minimized using AM1 Hamiltonian. To obtain more reliable results, the $\Delta H_{\mathrm{f}}^{0}$ values were calculated by using PECI = 8 formalism [18,19]. In this formalism, the

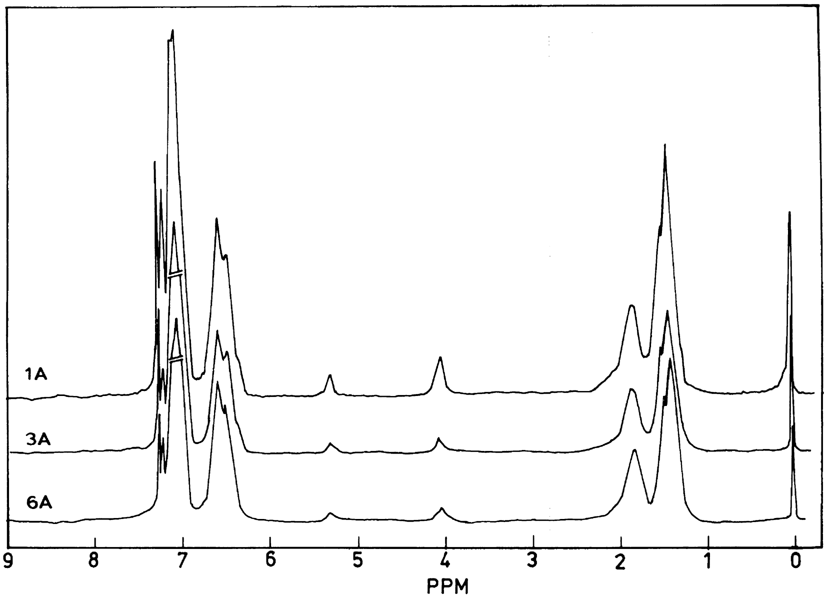

Fig. 1. ^{1}H NMR spectra of PS–PSP polymer produced at various time intervals (1A; $t = 3$ h); (3A; $t = 6$ h); (6A; $t = 12$ h).

minimized structures were used in the configuration interaction calculations, which included single and pair excitations involving eight frontier molecular orbitals. The degenerate sets of molecular orbitals were included for each radical.

4. Results and discussion

4.1. Synthesis and characterization of 'active' polymer

The polymerization of STY in the presence of Co(II)TPP(Py) and oxygen was accomplished at room temperature for various time intervals in a closed flask. The active polymer obtained was characterized by a ^{1}H NMR spectrum, which is displayed in Fig. 1. The peaks at 4.03 and 5.32 ppm correspond to the –CH$_2$‡ and >CH– of poly(styrene peroxide) (PSP) segments, respectively [20]. A doublet in the aromatic region ($\delta = 6.4$–7.5 ppm) as well as broad absorptions at 1.42 and 1.84 ppm arising from the –CH$_2$– and >CH– of polystyrene (PS) block [21], respectively, are observed. It was found that the concentration of both PSP and PS blocks in the backbone varies with the time of polymerization and their relative percentages are deduced by comparing the intensities of the –CH– peak of PSP (5.32 ppm) and PS (1.84 ppm) blocks. Fig. 2 presents the relative percentage of both PSP segments and PS formed with time. It is obvious that initially more PSP segments are formed and with time, owing to the decrease in concentration of oxygen in the reaction vessel, more PS is produced.

4.1.1. Mechanism of polymerization

Based on the results obtained, the mechanism of Co(II)TPP(Py) catalyzed polymerization of STY and MMA shown in Scheme 1 is proposed. To begin with, Co(II)TPP(Py) reacts with O_2 to form Co(III)TPP(Py)$^-$OO$^\bullet$ (Eq. (1)). The reactive Co(III) species then reacts with the monomer (Eq. (2)) thus initiating polymerization. The regenerated Co(II)TPP(Py) (Eqs. (2) and (3)) again initiates the polymerization. Such an initiation is reported in the literature for the formation of polyperoxides [16]. The possible propagation steps are shown in Eqs. (4)–(6). It is to be noted here that with time as the reaction proceeds the propagation through Eq. (6) predominates over Eq. (5) due

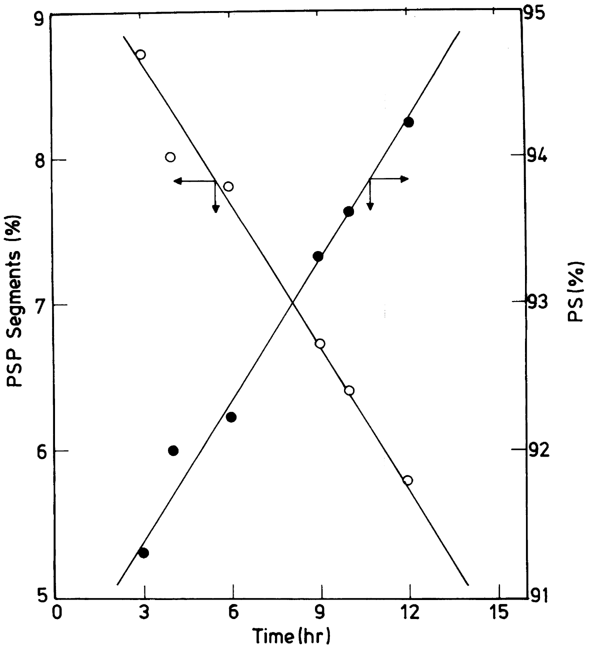

Fig. 2. Relative percentage of PSP and PS blocks obtained vs. time of polymerization of STY.

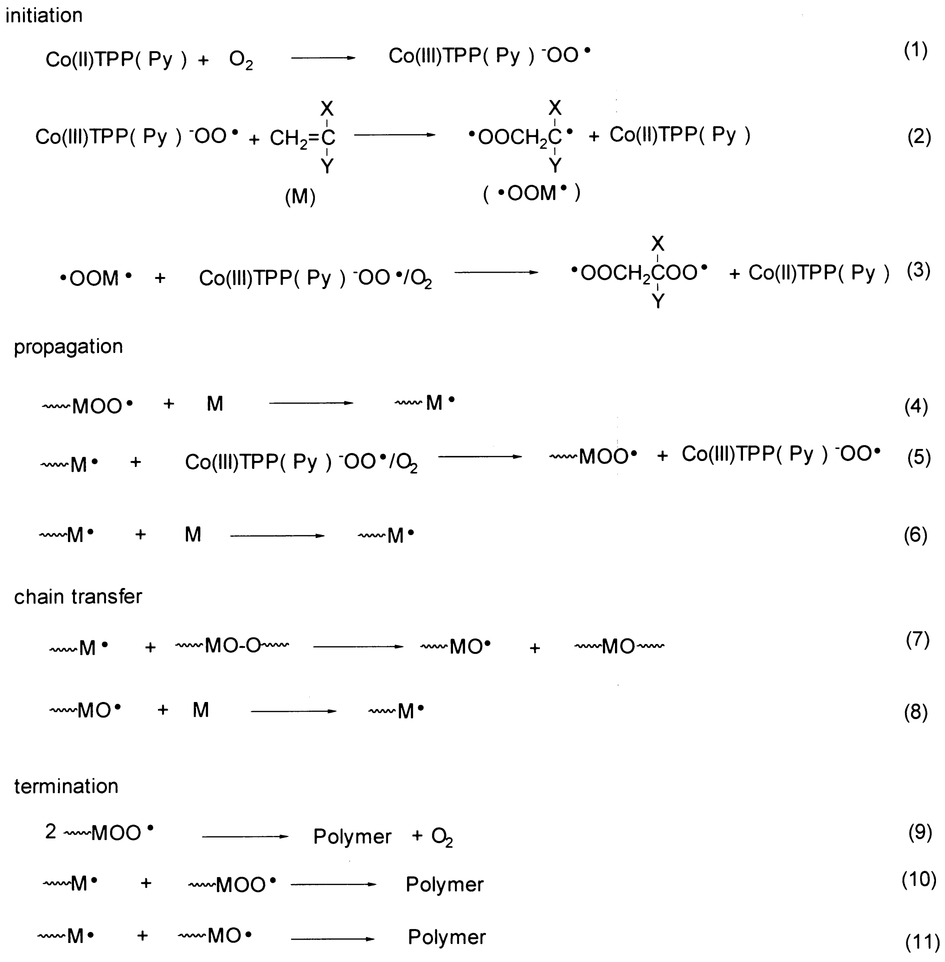

initiation

$$\mathrm{Co(II)TPP(Py)} + O_2 \longrightarrow \mathrm{Co(III)TPP(Py)}\,{}^{-}\mathrm{OO}^{\bullet} \quad (1)$$

$$\mathrm{Co(III)TPP(Py)}\,{}^{-}\mathrm{OO}^{\bullet} + \underset{(M)}{CH_2{=}\overset{X}{\underset{Y}{C}}} \longrightarrow \underset{(\bullet OOM^{\bullet})}{{}^{\bullet}OOCH_2\overset{X}{\underset{Y}{C}}{}^{\bullet}} + \mathrm{Co(II)TPP(Py)} \quad (2)$$

$$\bullet OOM^{\bullet} + \mathrm{Co(III)TPP(Py)}\,{}^{-}\mathrm{OO}^{\bullet}/O_2 \longrightarrow {}^{\bullet}OOCH_2\overset{X}{\underset{Y}{C}}OO^{\bullet} + \mathrm{Co(II)TPP(Py)} \quad (3)$$

propagation

$$\sim\!\!\sim MOO^{\bullet} + M \longrightarrow \sim\!\!\sim M^{\bullet} \quad (4)$$

$$\sim\!\!\sim M^{\bullet} + \mathrm{Co(III)TPP(Py)}\,{}^{-}\mathrm{OO}^{\bullet}/O_2 \longrightarrow \sim\!\!\sim MOO^{\bullet} + \mathrm{Co(III)TPP(Py)}\,{}^{-}\mathrm{OO}^{\bullet} \quad (5)$$

$$\sim\!\!\sim M^{\bullet} + M \longrightarrow \sim\!\!\sim M^{\bullet} \quad (6)$$

chain transfer

$$\sim\!\!\sim M^{\bullet} + \sim\!\!\sim MO\text{-}O\sim\!\!\sim \longrightarrow \sim\!\!\sim MO^{\bullet} + \sim\!\!\sim MO\sim\!\!\sim \quad (7)$$

$$\sim\!\!\sim MO^{\bullet} + M \longrightarrow \sim\!\!\sim M^{\bullet} \quad (8)$$

termination

$$2\sim\!\!\sim MOO^{\bullet} \longrightarrow \text{Polymer} + O_2 \quad (9)$$

$$\sim\!\!\sim M^{\bullet} + \sim\!\!\sim MOO^{\bullet} \longrightarrow \text{Polymer} \quad (10)$$

$$\sim\!\!\sim M^{\bullet} + \sim\!\!\sim MO^{\bullet} \longrightarrow \text{Polymer} \quad (11)$$

Scheme 1.

to the decrease in oxygen concentration. Consequently, the formation of PS block increases (Fig. 2). The propagating chain also undergoes chain transfer reactions with the O–O bonds, thus producing alkoxy radicals (Eq. (7)), which can also initiate the polymerization (Eq. (8)). The various termination processes are shown in Eqs. (9)–(11), by which the macrogrowing radical chains terminate resulting in the PS–PSP active polymer.

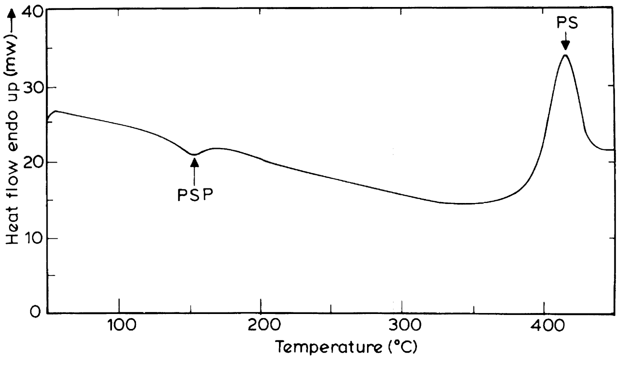

Fig. 3. DSC scan of PSP–PS of sample 2A.

4.1.2. Thermal analysis

The DSC and TGA curves of the PS–PSP active polymer are given in Figs. 3 and 4, respectively. In Fig. 3, the exotherm observed around 150°C and the broad endotherm in the range 390–415°C are due to the decomposition of the PSP segments [22] and the PS block, respectively. The TGA curve (Fig. 4) of the active polymer shows a two-step degradation. The initial small weight loss that occurs around 150°C and the large weight loss around 400°C are attributed to PSP segments [22,23] and PS block [24], respectively.

4.1.3. Molecular weight analysis

The conversion was 10% for the formation of the PS–PSP active polymer in 12 h. The molecular weights of the PS–PSP active polymers were determined using GPC analysis and the results are given in Table 1. All the polymers have very high molecular weights. Interestingly, the polydispersity obtained is much higher than that expected for a typical radical polymerization, which is 2. The broader polydispersity can be attributed to various types of chain transfer and termination reactions occurring in the present system. To get a theoretical value of 2, the termination reaction has to be a bimolecular disproportionation mechanism [25].

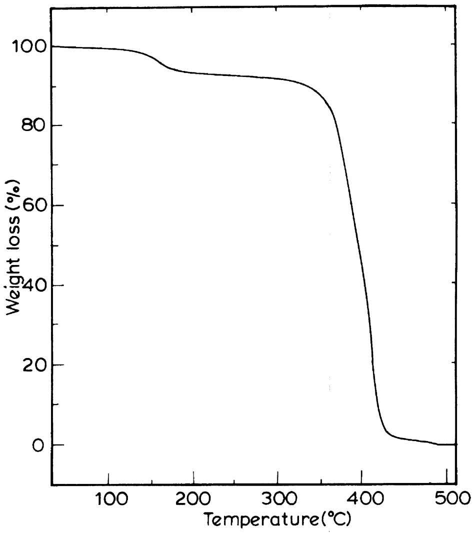

Fig. 4. TGA scan of PS–PSP of sample 2A.

Occurrence of other chain transfer and termination reactions will lead to deviation from the theoretical value [25].

To probe the polymerization process further, the number average molecular weight ($\bar{M}_n$) of PS–PSP was plotted against time (Fig. 5). The ($\bar{M}_n$) of PS–PSP increases linearly with time. However, it cannot be termed as a true living polymerization because of the wide polydispersity.

4.1.4. Polymerization of MMA

We have also applied the present technique for the polymerization of MMA and the polymer obtained was characterized by its ^{1}H NMR spectrum. The signals at δ 1.44, 3.76 and 4.34 ppm corresponded to α-CH_3, –OCH_3 and –OCH_2 of poly(methyl methacrylate peroxide) (PMMAP) segments, respectively [26], and those at 0.8–1.1, 1.89 and 3.65 ppm correspond to α-CH_3, –CH_2– and –OCH_3, respectively, of poly(methyl methacrylate) (PMMA) [21] block.

From Table 1, it may be seen that STY shows faster polymerization compared to MMA. The latter takes 72 h for the formation of active polymer PMMA–PMMAP (Table 1, run 1B). A comparison of $k_p/k_t^{1/2}$ (where k_p and k_t are the rate constants for the propagation and termination reactions, respectively) values for the oxidation of various vinyl monomers [27] reveals that when peroxy radicals are bonded to an electron-donating group, as in STY, the rate of oxidation is higher. On the other hand, when the electron-withdrawing group is attached to the peroxy radicals as in MMA, the rate of oxidation is rather low. Hence, in the present case, the formation of peroxy radicals and alkoxy radicals (formed by the degradation of peroxides) is faster for STY polymerization. Consequently, the rate of formation of active polymers, which are formed by the initiation of peroxy and alkoxy radicals, is faster for STY polymerization compared to MMA polymerization. The various reaction processes involved in the formation of active polymers are detailed in Scheme 1.

Table 1
Bulk polymerization of STY and MMA with Co(II)TPP(Py) ([Co(II)TPP(Py)] = 5.5 × 10^{-5} mol/l; [STY] = 8.69 mol l^{-1}; [MMA] = 9.42 mol l^{-1}; room temperature (27°C). 1A–6A: STY polymerization; 1B: MMA polymerization)

Run	Time (h)	$\bar{M}_n$ (× 10^{-4})	$\bar{M}_w$ (× 10^{-4})	$\bar{M}_w/\bar{M}_n$
1A	3	7.1	17.7	2.50
2A	4	8.1	20.5	2.53
3A	6	8.6	22.9	2.66
4A	9	9.7	27.7	2.86
5A	10	10.2	32.0	3.14
6A	12	11.1	32.5	2.93
1B	72	26.9	58.6	2.18

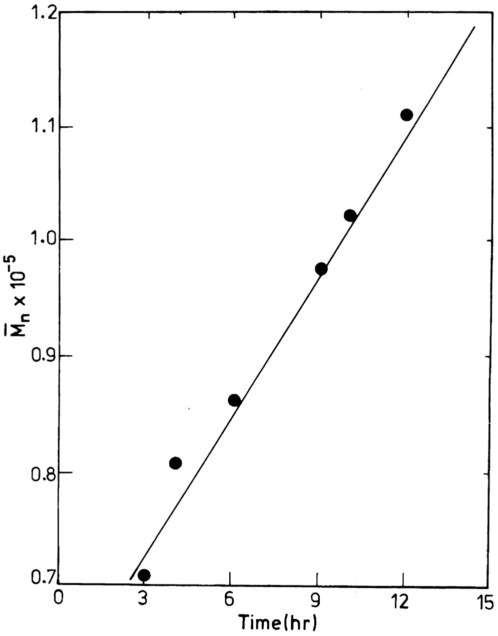

Fig. 5. Dependence of $\bar{M}_n$ with time of the polymerization of STY.

In order to emphasize the above fact further, the computational calculations on the heats of formation (ΔH_f^0) of the peroxy radicals of STY and MMA have been carried out. Here we have considered only the model radicals instead of actual macroradicals. The minimized conformations and the ΔH_f^0 values of STY and MMA peroxy radicals are presented in Fig. 6(a) and (b), respectively. The ΔH_f^0 of the peroxy radical of STY (15.1 kcal $mole^{-1}$) is very much higher than that of the MMA peroxy radical (-95.1 kcal $mole^{-1}$), suggesting that the former is more reactive than the latter.

It may be summarized that for the formation of active polymers in the case of STY polymerization, the rate of generation as well as the reactivities of the peroxy radicals (also the alkoxy radicals) are higher (owing to high $k_p/k_t^{1/2}$, and ΔH_f^0 values) compared to MMA polymerization (low $k_p/k_t^{1/2}$, and ΔH_f^0 values). Hence, the rate of formation of active polymers of STY is higher than that of MMA.

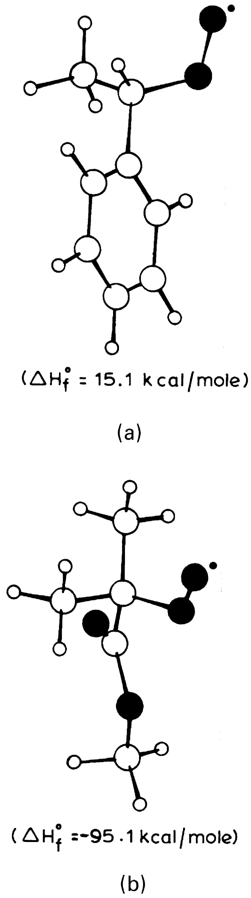

Fig. 6. Minimized conformations and heats of formation (ΔH_f^0) of: (a) STY peroxy, and (b) MMA peroxy radicals.

4.2. Metamorphosis of block-into-block copolymer

Although block copolymers could be synthesized using free radicals, the transformation of a block copolymer macroinitiator such as PS–PSP into another block copolymer namely PS-*b*-PMMA seems attractive, but is rarely reported. By using PS–PSP as a thermal initiator, PS was converted into the block copolymer PS-*b*-PMMA by the degradation of peroxide segments in the presence of the monomer MMA. The results for the block copolymerization of MMA using the active polymer, PS–PSP, is recorded in Table 2. It reveals some general features of this mode of block copolymerization. Active polymers used as initiators for block copolymerization show the conventional properties of peroxidic initiators. The conversion for the synthesis of the block copolymer at room temperature is lower (i.e. 13.3%) than at 80°C (20.9%). This may be a result of the formation of alkoxy radicals (generated by the cleavage of peroxy segments of the active polymer) and other reactions (detailed in Scheme 2, which shows the mechanism of formation of PS-*b*-PMMA), which are being facilitated at higher temperatures. Hence, the conversion (i.e. the quantity of block copolymer formation) increases at higher temperatures. Again, the percentage of conversion increases with increase in the concentration of the active polymer. The homo PS does not form under the reaction conditions employed for the synthesis of the active polymer, PS–PSP, demonstrating the importance of the present technique. Hence, all PS become active and get incorporated into the block copolymer.

4.2.1. Characterization

The absence of the characteristic PSP signals at δ 4.03 ($-CH_2OO-$) and 5.3 ($>CHOO-$) ppm in the ^1H NMR spectrum (Fig. 7) of the PS-*b*-PMMA showed the absence of any residual PSP segments in the backbone. The ^1H NMR spectrum of the block copolymer, exhibiting the characteristic signals of PS at 1.42 ($-CH_2-$), 1.84 ($>CH-$), 6.4–6.6 (*o*-protons) and 7.2 ppm (*p*- and *m*-protons); and of PMMA at 0.8–1.1 ($-CH_3$), 1.89 ($-CH_2-$) and 3.65 ppm ($-OCH_3$) support the formation of PS-*b*-PMMA.

4.2.2. Thermal analysis of PS-*b*-PMMA

The TG thermogram (Fig. 8) of PS-*b*-PMMA shows a two-step weight loss. The first step is due to the degradation of the PMMA block [28] and the other step corresponds to the degradation of the PS block [24,29]. The TGA thermograms of the PMMA block correlates with its endothermic degradation of the DSC scan [30]. There is no weight loss around 150°C, indicating the absence of any residual PSP segments in the block copolymer.

Table 2
Block copolymerization with MMA by PS–PSP active polymer

Run	PS–PSP[a] (wt%)	Conversion of comonomer (wt%)	Extraction (wt%)		
			Homo PS	Homo PMMA	PS-*b*-PMMA
I	4.1	13.3	0	34	66
II	4.1	20.9	0	38	62
III	7.9	32.5	0	40	60
IV	11.4	43.2	0	37	63
V	14.6	55.3	0	40	60
VI	24.3	82.3	0	38	62

[a] Sample 5A of Table 1; [MMA] = 9.4 mol l^{-1}; PSP content (%) = 6.4; I: room temperature (27°C), time = 5 days; II–VI: temperature = 80°C, time = 5 h.

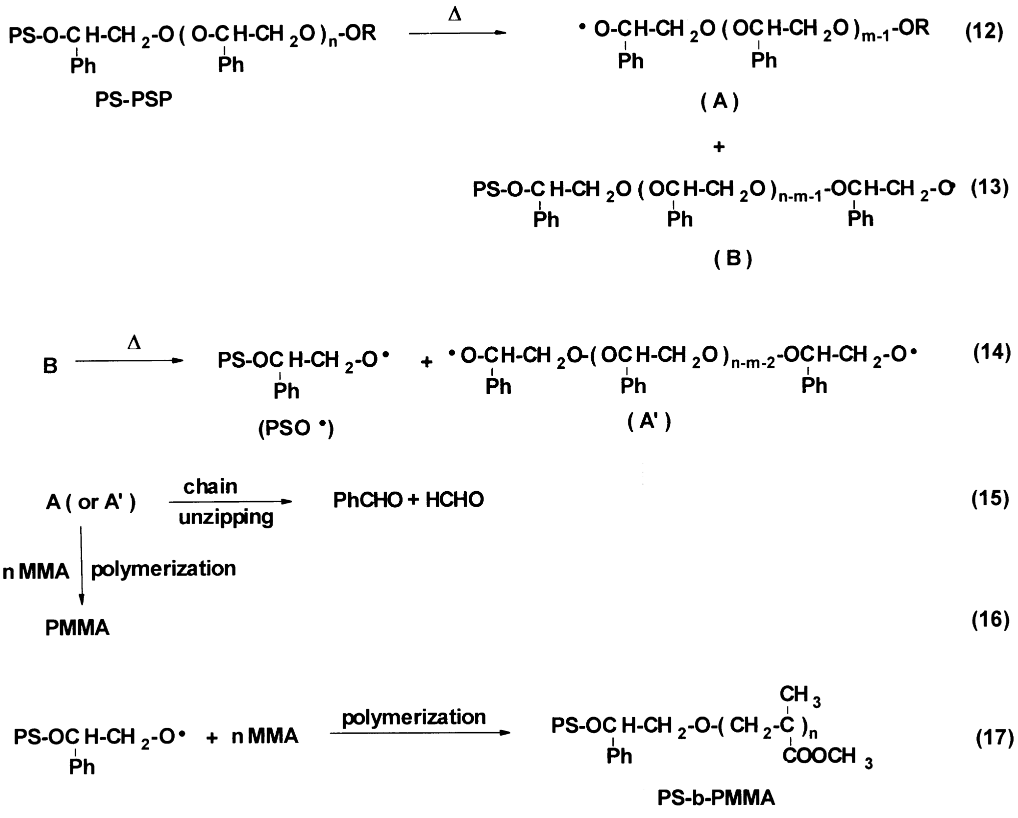

Scheme 2.

4.2.3. Mechanism of PS-*b*-PMMA formation

The steps involved in the PS-*b*-PMMA formation using PS–PSP active polymer are outlined in Scheme 2. The PS–PSP on heating generates β-peroxy alkoxy radicals, A and B (Eqs. (12) and (13)). The radical 'B' undergoes further dissociation producing poly(α-styrenyloxy) ($\mathrm{PSO}^{\cdot}$) and β-peroxy alkoxy radical, A' (Eq. (14)). The alkoxy radical, A (A') may undergo a chain unzipping reaction, giving benzaldehyde and formaldehyde (Eq. (15)) or react with MMA produced in the generation of PMMA homopolymer (Eq. (16)). The $\mathrm{PSO}^{\cdot}$ thus formed adds to MMA, resulting in the formation of PS-*b*-PMMA block copolymer (Eq. (17)).

The unzipping of alkoxy radicals to non-radical products (Eq. (15)) is thermodynamically more favorable (i.e. the heat of reaction $(\Delta H_r^0) = -80.7\ \mathrm{kcal\ mole}^{-1}$) than their addition to the monomer ($\Delta H_r^0 = -17.5\ \mathrm{kcal\ mole}^{-1}$) (Eq. (16)) [31]. Kinetically too, the latter process requires more activation energy than the unzipping reaction [31–33] and thus the unzipping process is much faster than the addition of the alkoxy radicals to the double bond. Hence, although

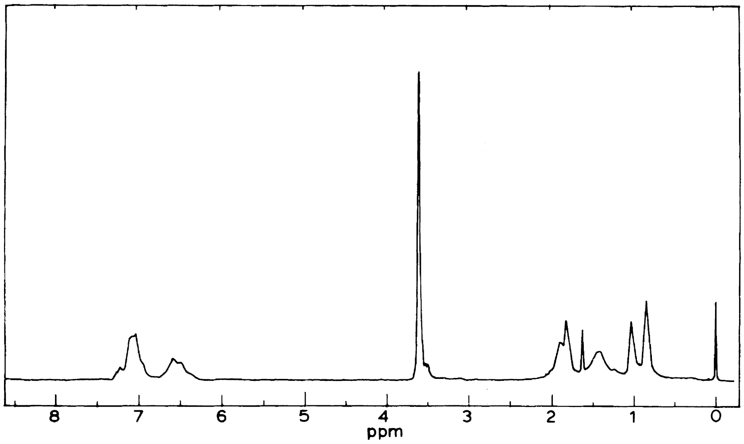

Fig. 7. ^{1}H NMR spectrum of PS-*b*-PMMA.

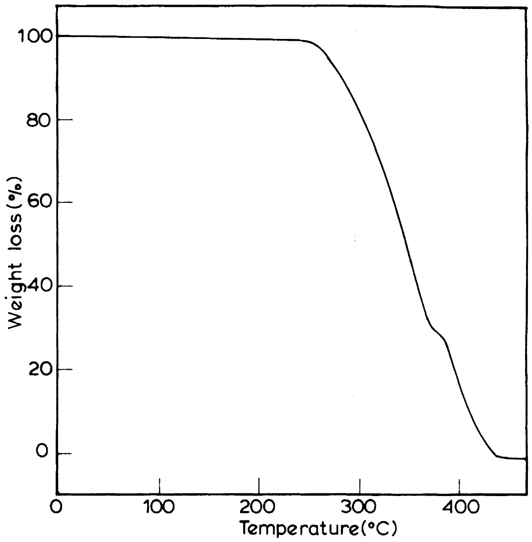

Fig. 8. TGA scan of PS-*b*-PMMA.

peroxides (i.e. PSP segments) are present, the quantity of homo PMMA produced is less in the product (Table 2).

5. Conclusions

It may be concluded that catalytic free-radical polymerization is a novel method for the polymerization of vinyl monomers at room temperature. The time taken for the formation of active polymers mainly depends upon the generation as well as the reactivities of their peroxy and alkoxy radicals. The initiating efficiency of PS–PSP has been determined in the synthesis of a common block copolymer, PS-*b*-PMMA. Vinyl polyperoxides are inexpensive materials since they can be made by reacting a vinyl monomer with air. Further, the synthesis is easy and less hazardous compared to acid polyperoxides [34]. Thus, vinyl polyperoxides are attractive as initiators.

Acknowledgements

A.K.N. thanks Prof. D.N. Sathyanarayana, Dr K. Ganesh and J. Jayaseheran for fruitful discussions.

References

[1] Moad G, Soloman DH. The chemistry of free-radical polymerization. Oxford: Pergamon Press, 1995.
[2] Ramelow U, Baysal B. Polymer 1986;27:949.
[3] Kishore K, Sanathlakshmi KN. J Polym Sci Polym Chem Ed 1981;19:2367.
[4] Kishore K, Bhanu VA. J Polym Sci Polym Chem Ed 1986;24:379.
[5] Tatsukami Y, Takahashi T, Yoshioka H. Makromol Chem 1980;181:1107.
[6] Fordham JW, Williams HL. J Am Chem Soc 1951;73:1634.
[7] Orr RJ, Williams HL. J Am Chem Soc 1955;77:3715.
[8] Orr RJ, Williams HL. J Phys Chem 1953;57:925.
[9] Odian G. Principles of polymerization. 3rd ed. New York: Wiley, 1991 (p. 219).
[10] Bates FS. Science 1991;251:898.
[11] Trollsas M, Hedrick JL. J Am Chem Soc 1998;120:4644.
[12] Hedrick JL, Carter KR, Labadie JW, Miller RD, Volksen W, Hawker C, Yoon DY, Russell TP, McGrath JE, Briber RM. Adv Polym Sci 1999;141:1.
[13] Aggrawal SL. Block copolymers. New York: Plenum Press, 1970.
[14] Yamashita Y. Chemistry and industry of macromonomers. Tokyo: IPC, 1984 (p. 1).
[15] Perrin DD, Armarego WLF. Purification of laboratory chemicals. Oxford: Pergamon Press, 1988.
[16] Jayaseheran J, Kishore K. J Am Chem Soc 1998;120:825.
[17] Rauhut G, Alex A, Chandrasekhar J, Steinke T, Sauer W, Beck B, Hutter M, Gedeck P, Clark T. VAMP 6.0. Oxford Molecular Ltd, The Medawar Centre, Oxford Science Park, Oxford OX4 4GA, England, 1996.
[18] Dewar MJS, Zeobisch EG, Healy EF, Stewart JJP. J Am Chem Soc 1985;107:3902.
[19] Clark T, Chandrasekhar J. Isr J Chem 1993;33:435.
[20] Cais RE, Bovey FA. Macromolecules 1977;10:169.
[21] Pham QT, Petiaud R, Waton H. Proton and carbon NMR spectra of polymers. New York: Wiley, 1983.
[22] Kishore K, Mukundan T. Nature 1986;324:130.
[23] Jayaseheran J, Nanda AK, Kishore K. Polymer 2000;41:5721.
[24] Jang LW, Lee DC. Polymer 2000;41:1749.
[25] Ward TC. J Chem Ed 1981;58:867.
[26] Mukundan T, Kishore K. Macromolecules 1987;20:2382.
[27] Mogilevich MM. Russ Chem Rev 1979;48(2):199.
[28] Cimmino S, Iodice P, Silvesftre C, Karasz FE. J Appl Polym Sci 2000;7:746.
[29] Otsu T, Yoshida T. Polym Bull 1982;7:197.
[30] Yamamoto T, Aoshima K, Ohmura H, Moriya Y, Suzuki N, Oshibe Y. Polymer 1991;32:19.
[31] Nanda AK, Kishore K. Ind J Chem Sec A 2000;39A:631.
[32] Mayo FR. J Am Chem Soc 1958;80:2465.
[33] Nanda AK, Ganesh K, Kishore K, Surinarayan M. Polymer 2000;41:9063.
[34] Hazer B, Baysal BM. Polymer 1986;27:961.